No. 1A-11 $PbTiO_3$, Lead titanate
(M = 303.1)

1a Ferroelectric activity was suggested independently by Shirane et al. and Smolenskii in 1950. 50Shi, 50Smo

b

phase	II	I
state	F	P
crystal system	tetragonal	cubic
space group	P4mm – C_{4v}^1	Pm3m – O_h^1
Θ [°C]	490	

46Meg, 51Shi2

The other phase transitions were reported to occur at about −100 °C, −160 °C or −90 °C in X-ray [a]) and optical [b]) measurements; 55Kob, 69Ike, 73Dos, 83Kob

T_{melt} = 1281(3) °C. $\rho = 7.96(1)\cdot 10^3\ kg\,m^{-3}$. 52Rog

P_s || [100]. 46Meg

2a Crystal growth: flux method [a]), Bridgman-Stockbarger method [b]), Czochralski method [c]), hydrothermal method [d]), sol-gel process [e]). [a])52Nom, 58Kob, 70Rem, 93Sun; [b])52Rog; [c])76Gra; [d])63Chr, 65Kuz, 68Sht; [e])85Blu

Amorphous preparation: twin-roller quenching method. 80Tak

Phase diagram of $PbO–TiO_2$: Fig. 1A-11-001.

Non-stoichiometric $PbTiO_3$ compounds are prepared. 71Shi, 73Shi, 75Shi

3a Positional parameters: Table 1A-11-001, Table 1A-11-002. 61Ste

Unit cell parameters: Table 1A-11-003; see also 79Mab

b Projection of crystal structure: Fig. 1A-11-002, Fig. 1A-11-003.

Atomic displacements: Table 1A-11-003; Fig. 1A-11-004.

4 Thermal expansion: Figs. 1A-11-005...1A-11-010, see also 68Bhi

Dependence of lattice parameters on hydrostatic pressure: Fig. 1A-11-011, Fig. 1A-11-012, see also 62Kab

5a Dielectric constant: Fig. 1A-11-013, Fig. 1A-11-014, see also 79Mal, 81Oku

Small dielectric anomaly was observed at about −100 and −150 °C. 56Kob

Curie-Weiss constant: $C = 4.1\cdot 10^5$ °C. Because of its high Curie temperature, the Curie-Weiss constant varies to some extent, depending on the crystal and measuring method. 70Shi, 70Rem

Effect of p on κ: Figs. 1A-11-015...1A-11-017.

Phase diagram in regard to p: Fig. 1A-11-018.

	$[d\Theta_{II-I}/dp]_{p=0} = -8.4(3)\cdot10^{-8}$ K Pa^{-1} $[d\Theta_p/dp]_{p=0} = -7.1(3)\cdot10^{-8}$ K Pa^{-1} $[dC/dp]_{p=0} = -9.1(7)\cdot10^{-5}$ K Pa^{-1}	71Sam
c	Spontaneous polarization: Fig. 1A-11-019.	
	The theoretical value of P_s was estimated to be $8.1\cdot10^{-1}$ Cm^{-2} by Venevtsev et al.	59Ven
	The semiempirical value to be $6.6\cdot10^{-1}$ Cm^{-2} by Bhide et al.	68Bhi
	Effect of electric field on dielectric constant: see	95Fon
	Spontaneous polarization and coercive field: spontaneous polarization and coercive field obtained from the D–E hysteresis are $7.5\cdot10^{-1}$ Cm^{-2} and $6.75\cdot10^{5}$ Vm^{-1} for single crystal and $8.0\cdot10^{-1}$ Cm^{-2} and $2.8\cdot10^{7}$ Vm^{-1} for thin film, respectively.	70Gav 93Tab 94Gav
	Spontaneous polarization of $80\pm1\cdot10^{-1}$ Cm^{-2} has been reported in single crystal having single domain; see also Fig. 1A-11-004 and	70Rem 79Mal
d	Pyroelectricity: Figures of merit for infrared detector are given.	71Yam, 76Yam
	Pyroelectric coefficient: Fig. 1A-11-020.	
6a	Heat capacity: Fig. 1A-11-021, Fig. 1A-11-022.	
	II-I: $\Delta Q_m = 4807$ J mol^{-1}, $\Delta S_m = 6.7$ J K^{-1}mol^{-1}.	51Shi
	DTA: Small exothermic and endothermic anomalies are observed near 113 K in the cooling and heating process.	69Ike
c	Thermal conductivity: Fig. 1A-11-023.	
7a	Piezoelectric properties: Table 1A-11-004, Table 1A-11-005; Figs. 1A-11-024...1A-11-030.	
9a	Refractive indices: $n_o = 2.6676$, $n_e = 2.6594$ for $\lambda = 0.6328$ μm.	71Pre
	n was fitted to the dispersion equation $n^2 - 1 = E_d E_o/(E_o^2 - E^2)$ for λ between 0.45 and 1.15 μm, where $E_d = 29.66$ eV and $E_o = 5.53$ eV for n_o, $E_d = 30.64$ eV and $E_o = 5.71$ eV for n_e, and E is the photon energy in eV, E_o: oscillator energy, E_d: dispersion energy. Fig. 1A-11-031, Fig. 1A-11-032; see also	72Sin 79Mab
	Birefringence: Figs. 1A-11-033...1A-11-035.	87Mal
	Infrared reflection and absorption: Figs. 1A-11-036...1A-11-040. Frequencies of infrared modes: Table 1A-11-006.	
	Optical absorption: Fig. 1A-11-041, Fig. 1A-11-042.	92Zha
b	Electrooptic effect: $r^{S}_{13} = 13.8\cdot10^{-12}$ mV^{-1}, $r^{S}_{33} = 5.9\cdot10^{-12}$ mV^{-1} for $\lambda = 0.633$ μm.	71Pas
d	Gyration tensor: Fig. 1A-11-034.	
e	Nonlinear optical susceptibilities: Fig. 1A-11-043.	
	$d_{15}/\lvert d_{11}^{quartz}\rvert = \mp 104.1(157)$, $d_{31}/\lvert d_{11}^{quartz}\rvert = \mp 117.6(176)$, $d_{33}/\lvert d_{11}^{quartz}\rvert = \pm 23.4(38)$ for $\lambda = 1.064...1.319$ μm.	72Sin
	Second harmonic generation: see Fig. 1A-2-025 in No. 1A-2, $KNbO_3$.	
10	Raman scattering: Figs. 1A-11-044...1A-11-048; see also	70Tak
	Damping of the soft E-symmetry phonon: see	78Hei
	Effect of pressure on the zone-center phonons: Fig. 1A-11-049, Fig. 1A-11-050.	
	For amorphous specimen: see	81Nak, 84Nak
11	Conductivity: Fig. 1A-11-051.	
	The conductivity of ceramics is $10^{-5}...10^{-6}$ Ω^{-1}m^{-1} at RT but very much dependent on the sintering condition of the ceramics. Also, effect of some impurities on the conductivity is seen.	69Gur 76Pro

	Seebeck effect: Fig. 1A-11-052.	
	Photoconductivity: the maximum at $\lambda \approx 410$ nm.	76Mal
	Electronic structure was calculated by PβX_α method [a]), ultra-soft-pseudopotential method [b]), LCAO method [c]).	[a])81Roz, 83Shv [b])94Kin [c])92Pro
	Photoconductivity: see	83Rae
13b	ESR: Fe^{3+}, Spin-Hamiltonian parameters at −188 °C. For narrow line width spectrum: $D = 118.7(2)$ m^{-1}, $a = 2.0(7)$ m^{-1}, $F = -1.7(10)$ m^{-1}. For wide line width spectrum: $D = 115.0(3)$ m^{-1}, $a = 2.2(10)$ m^{-1}, $F = -2(1)$ m^{-1}. Table 1A-11-007. Mn^{2+}: Table 1A-11-008. Fig. 1A-11-053; see also	76Lew 85Bal
c	Mössbauer effect: Figs. 1A-11-054...1A-11-057. Additional informations can be found in Perturbed γ–γ directional correlation for the first excited state of ^{44}Sc in $PbTiO_3$ at −189 °C: $\lvert QV_{zz}\rvert = 4.09(9)\cdot 10^{-8}$ V.	 69Yam, 71Yag 73Dos
14b	Inelastic neutron scattering: Figs. 1A-11-058...1A-11-060.	
c	EXAFS: Fig. 1A-11-061; see also	81Ter, 94Sic
15a	Domain structure: see	52Nom, 58Kob, 59Kob, 68Bhi, 72Fes, 73Fes, 75Tan
b	Domain switching: the mobility of side motion ranges from 10^{-8} to 10^{-7} m^{2}V^{-1}s^{-1}.	76Fes
16	Surface layer: X-ray diffraction measurements under d.c. electric field show the existence of a surface layer with thickness of about $1.04\cdot 10^{-6}$ m. Radiation damage: Fig. 1A-11-062. Thin film growth: RF sputtering, chemical vapor deposition, laser annealing. Thin film dielectric property: see Fig. 1A-11-014 in 5a and Fig. 1A-11-020 in 5d; see also	74Dud, 78Dud 79Oku, 83Koj, 81Mat 81Oku, 85Shi, 86Iij

Table 1A-11-001. $PbTiO_3$. Fractional coordinates of atoms in the unit cell of phase II at RT [56Shi].

Atom	*x*	*y*	*z*
Pb	0	0	0
Ti	1/2	1/2	0.540
O(1)	1/2	1/2	0.112
O(2)	1/2	0	0.612
	0	1/2	0.612

Table 1A-11-002. $PbTiO_3$. Bond lengths [in Å] in phase II at RT and in phase I at 490 °C [56Shi]. $O(1)_+$ and $O(1)_-$ represent the O(1) atoms closer to and further away from Ti atom, respectively. Similarly $O(2)_+$ is closer to Pb atom.

Phase	II (at RT)	I (at 490°C)
Ti–$O(1)_+$	1.78	1.89
Ti–$O(1)_-$	2.38	
Ti–O(2)	1.98	
Pb–O(1)	2.80	2.80
Pb–$O(2)_+$	2.53	
Pb–$O(2)_-$	3.20	

Table 1A-11-003. $PbTiO_3$. Refined structural parameters for tetragonal $PbTiO_3$ at 295 K and 700 K [85Nad]. δ_z: displacements of atoms from the cubic phase sites (in fraction). U_{ij}: the mean-square thermal amplitudes (in $Å^2$ units) in the unit cell of phase II. U_{ij} are defined by Eq. (d) in Introduction. *a*, *c*: lattice constants. R_w: final weighted *R*-factor.

		$T = 295$ K	$T = 700$ K
Pb	U_{11} [$Å^2$]	0.0089(2)	0.0231(3)
	U_{22} [$Å^2$]	0.0083(2)	0.0226(3)
Ti	δ_z	0.0377(4)	0.0250(4)
	U_{11} [$Å^2$]	0.0037(3)	0.0090(3)
	U_{33} [$Å^2$]	0.0054(5)	0.0118(7)
OI	δ_z	0.1118(3)	0.0799(4)
	U_{11} [$Å^2$]	0.0095(2)	0.0207(3)
	U_{33} [$Å^2$]	0.0055(3)	0.0098(3)
OII	δ_z	0.1174(3)	0.0845(4)
	U_{11} [$Å^2$]	0.0081(2)	0.0197(3)
	U_{22} [$Å^2$]	0.0039(2)	0.0081(2)
	U_{33} [$Å^2$]	0.0095(2)	0.0203(3)
	a [Å]	3.902(3)	3.940(6)
	c [Å]	4.156(3)	4.063(6)
	R_w	0.025	0.036

Table 1A-11-004. $PbTiO_3$. Physical constants at RT.

	Single crystal [71Gav]	Ceramics [a]) [71Ike] [b])
a [Å]		3.9072
c [Å]		4.1187
Θ_f [°C]		470
ρ_{exp} [$\cdot 10^3$ kg m^{-3}]	7.9	7.87
Porosity [%]		1.5
ρ [Ωm]		$2 \cdot 10^{10}$
Dielectric constants		
κ_{11}^{T}	210	1 kHz 230
κ_{11}^{S}	115	210
κ_{33}^{T}	126	1 kHz 170
κ_{33}^{S}	51	140
Dissipation factor D		0.008
Frequency constants		
N_p [Hz m]		2640
N_{31}		2050
N_{33}		2020
N_t		2070
N_{15}		1340

	Single crystal [71Gav]	Ceramics [a]) [71Ike] [b])
Elastic constants		
s_{11}^{E} [$\cdot 10^{-12}$ m^2 N^{-1}]	7.2	7.5
s_{12}^{E}	–2.1	–1.5
s_{13}^{E}		–1.1
s_{33}^{E}	32.5	8.0
s_{44}^{E}	12.2	17.9
s_{11}^{D}		7.5
s_{12}^{D}		–1.5
s_{13}^{D}		–1.1
s_{33}^{D}		6.4
s_{44}^{D}		16.5
s_{66}	7.9	18.0
c_{33}^{E} [$\cdot 10^{10}$ Nm^{-2}]		13.1
c_{33}^{D}		16.6
Poisson's ratio σ^E		0.20
Mechanical quality factor Q		1100

[a]) 1.25 mol% La_2O_3, 1.0 mol% MnO_2. [b]) See also [72Ued].

Table 1A-11-005. $PbTiO_3$. Electromechanical constants at RT.

	Single crystal [71Gav]	Ceramics (1.25 mol% La_2O_3, 1.0 mol% MnO_2) [71Ike] [a])
Coupling factors		
k_p	0.40	0.07
k_{31}	0.24	0.04
k_{33}	0.64	0.46
k_t		0.46
k_{15}	0.43	0.28
Piezoelectric constants		
d_{31} [$\cdot 10^{-12}$ C N^{-1}]	–2.5	–4.4
d_{33}	11.7	51
d_{33} [b])	19.3	
d_{15}	6.5	53
g_{31} [$\cdot 10^{-3}$ m^2C^{-1}]		–2.9
g_{33}		33
g_{15}		27
Electrostrictive constants for P		
Q_{11} [m^4C^{-2}]	0.080	
Q_{12}	–0.029	

[a]) See also [72Ued]. [b]) Static method.

Table 1A-11-006. $PbTiO_3$. Wave numbers in 10^2 m^{-1} and symmetries of infrared modes of lattice vibration obtained from Kramers-Kronig analysis of the reflectance data at RT [65Per].

$\tilde{\nu}_1$ (Ti–O stretch)	$\tilde{\nu}_2$ (Ti–O_3 torsion)	$\tilde{\nu}_3$ (O–Ti–O bend)	$\tilde{\nu}_4$ (cation–TiO_3 lattice mode)
530 (E_u, A_1)	400 (B_1, E_u)	220 (E_u, A_1) 172	83 (E_u, A_1)

Table 1A-11-007. $PbTiO_3$. *g*-factor at RT [64Gai].

Paramagnetic center	Site	*S*	**H**	*v* [GHz]	*T* [K]	$g_{\parallel}$	$g_{\perp}$
Fe^{3+}	Ti^{4+}	1/2 *)	(2)	8.8	RT	2.009(5)	5.97(2)

*) Observed spectrum could be described by effective spin of 1/2, which was explained in terms of a strong tetragonal component of the crystalline field.

Table 1A-11-008. $PbTiO_3$. ESR data [69Ike].

Paramagnetic center	Mn^{2+}
Site	Ti^{4+}
S	5/2
H	(7)
ν [GHz]	≈9

	Cubic phase	Tetragonal phase
g-factor	1.996(2)	2.084(2)
FS [$\cdot 10^{-2}$ m^{-1}]	$D = 0$	$D = +\ 502(4)$
	–	$a = +\ 43(2)$
HFS [$\cdot 10^{-2}$ m^{-1}]	−79.8(5)	−82.0(15)

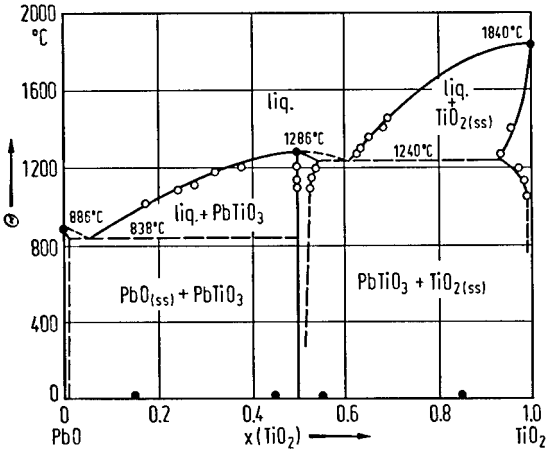

Fig. 1A-11-001. $PbTiO_3$. Phase diagram of system $(PbO)_{1-x}(TiO_2)_x$ [76Hol]. Refined by mass-loss Knudsen effusion. Full circles: DTA, open circles: mass-loss Knudsen effusion.

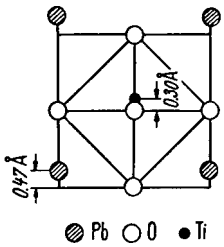

Fig. 1A-11-002. $PbTiO_3$. Projection of the structure of phase II along the *a*-axis [56Shi].

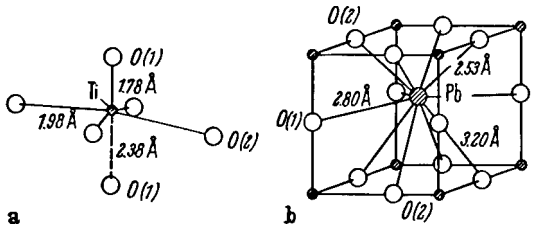

Fig. 1A-11-003. $PbTiO_3$. A sketch of the structure of phase II at RT [56Shi]. (**a**) environment of Ti atom, (**b**) environment of Pb atom.

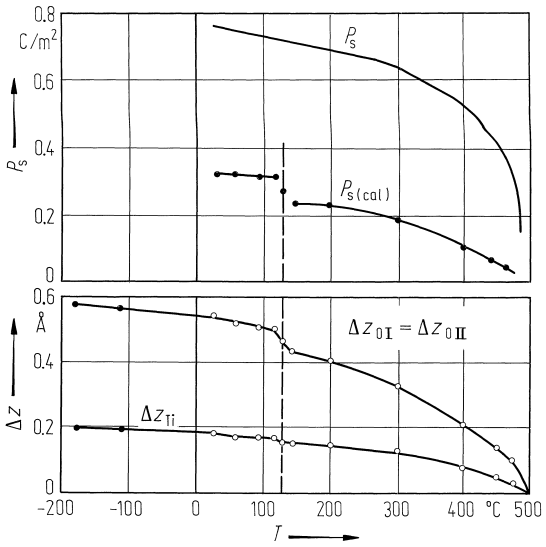

Fig. 1A-11-004. $PbTiO_3$. Δz and P_s vs. T [83Kup]. Δz: atomic displacement. P_s(cal): spontaneous polarization due to the displacement of cation from the center of oxygen octahedron. Full circles: data from [78Gla].

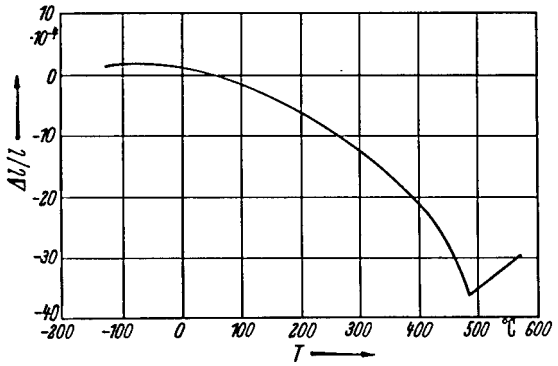

Fig. 1A-11-005. $PbTiO_3$ (ceramics). $\Delta l/l$ vs. T [51Shi1].

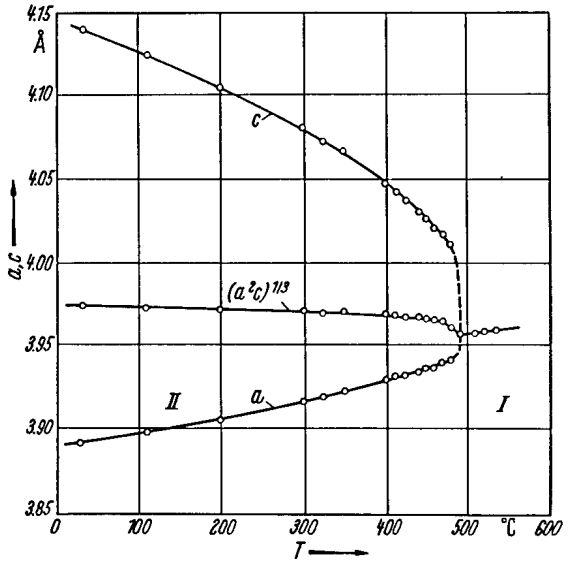

Fig. 1A-11-006. $PbTiO_3$. Lattice constants *a*, *c* vs. *T* [51Shi1].

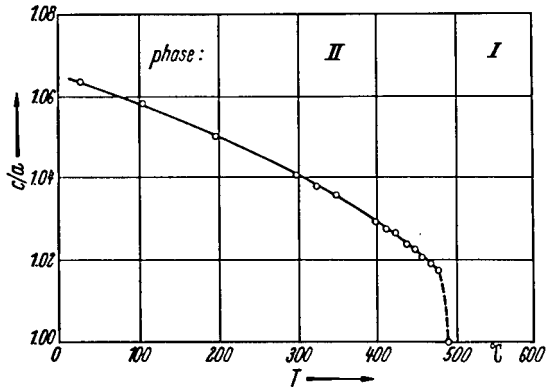

Fig. 1A-11-007. $PbTiO_3$. *c/a* vs. *T* [51Shi1]. *c*, *a*: lattice constants.

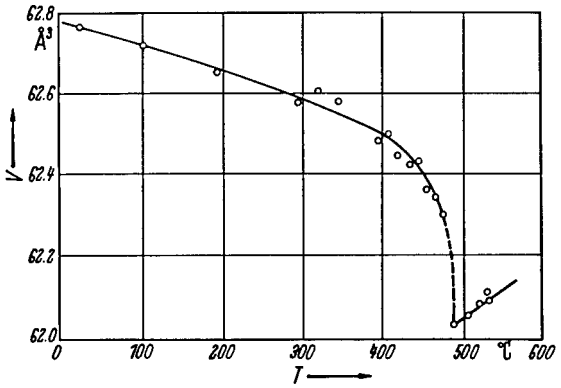

Fig. 1A-11-008. $PbTiO_3$. *V* vs. *T* [51Shi1]. *V*: unit cell volume.

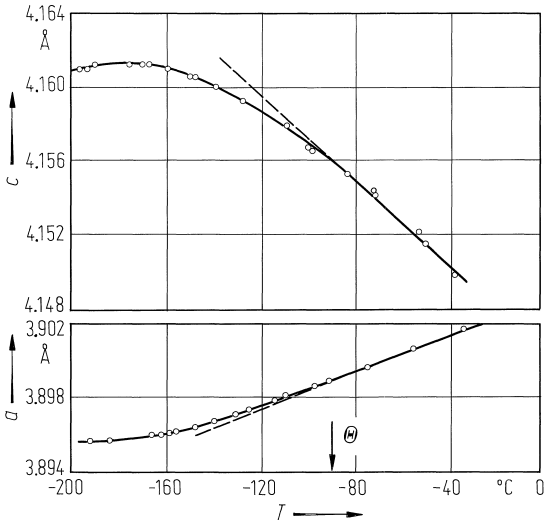

Fig. 1A-11-009. $PbTiO_3$. Lattice constants *a*, *c* vs. *T* [83Kac].

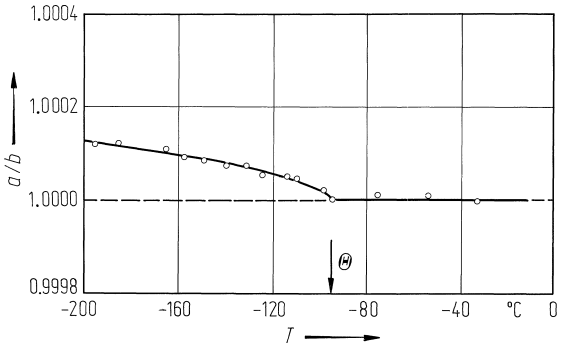

Fig. 1A-11-010. $PbTiO_3$. *a/b* vs. *T* [83Kac].

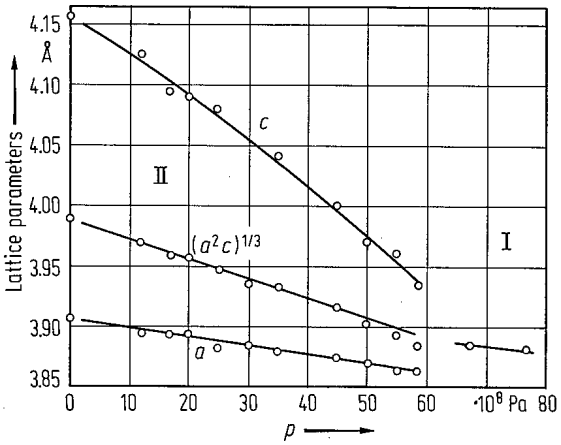

Fig. 1A-11-011. $PbTiO_3$. Lattice constants *a*, *c* vs. *p* [75Ike].

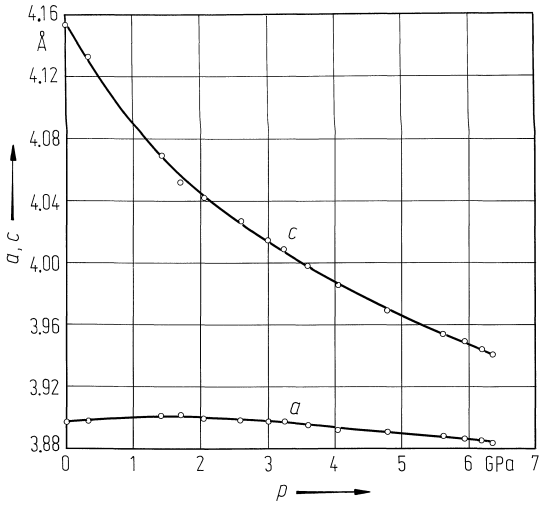

Fig. 1A-11-012. $PbTiO_3$. *a*, *c* vs. *p* at *T* = 292 K [86Nel].
p: hydrostatic pressure.

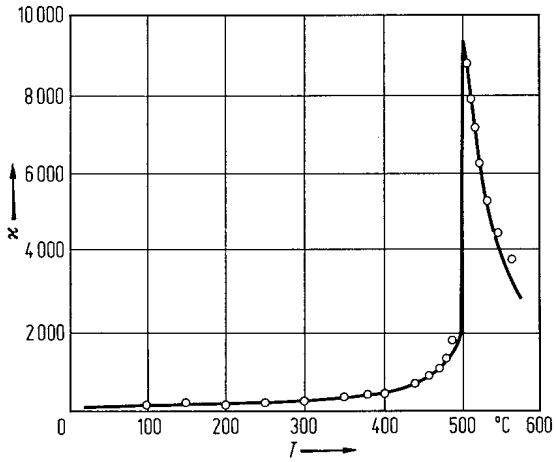

Fig. 1A-11-013. $PbTiO_3$. κ vs. T [70Rem].

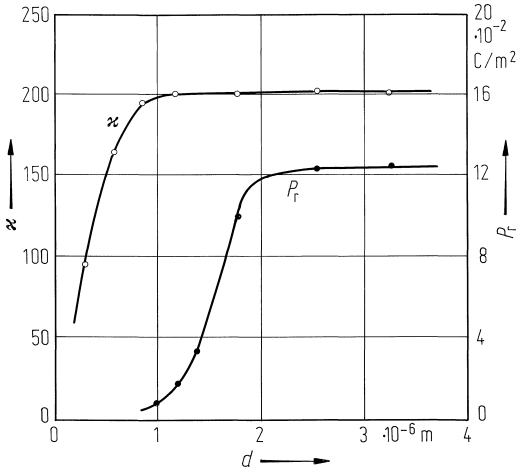

Fig. 1A-11-014. $PbTiO_3$ (thin film). κ, P_r vs. d [81Oku]. d: film thickness.

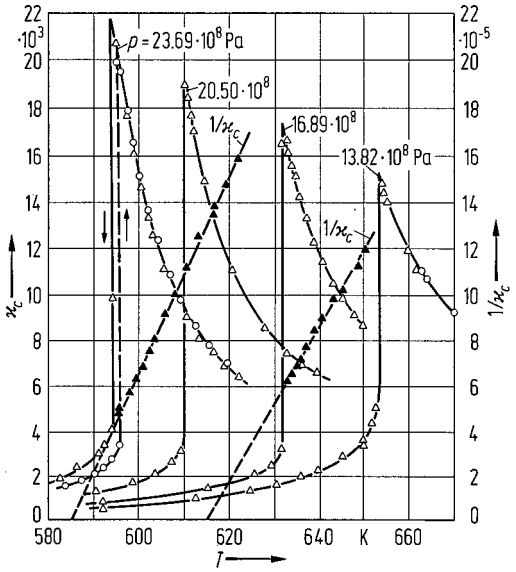

Fig. 1A-11-015. $PbTiO_3$. κ_c, $1/\kappa_c$ vs. T [71Sam]. Parameter: p.

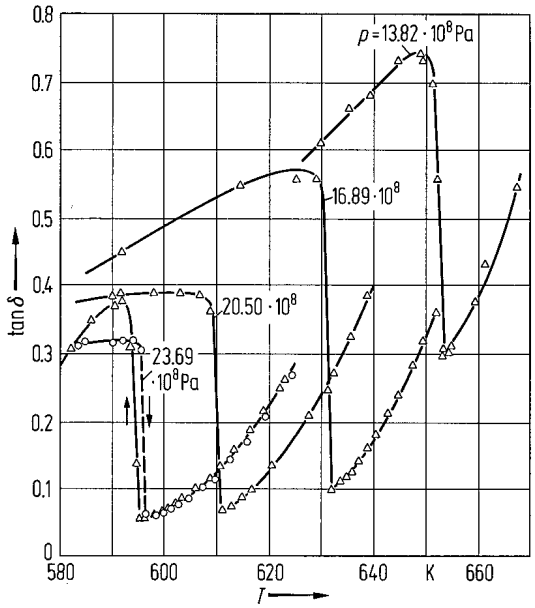

Fig. 1A-11-016. $PbTiO_3$. tan δ vs. T [71Sam]. Parameter: p.

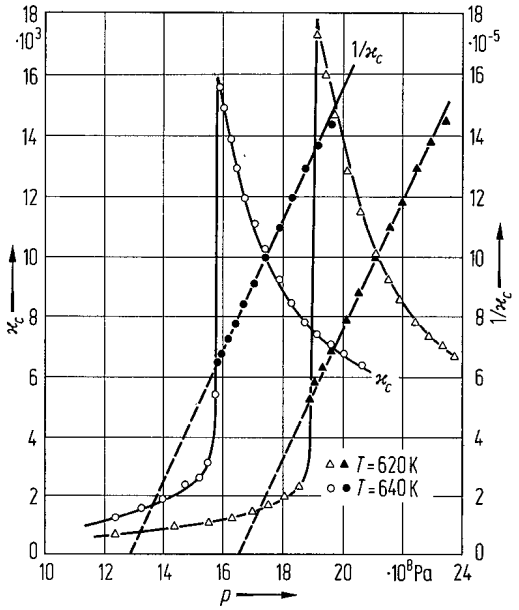

Fig. 1A-11-017. $PbTiO_3$. κ_c, $1/\kappa_c$ vs. p [71Sam].

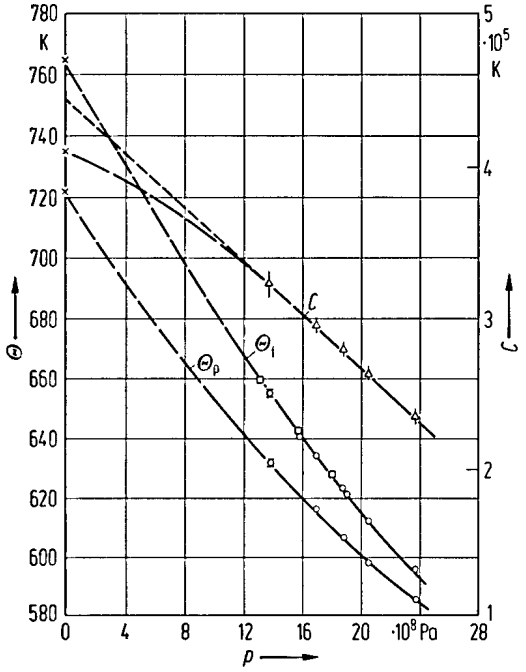

Fig. 1A-11-018. $PbTiO_3$. Θ_p, Θ_f, C vs. p [71Sam].
C: Curie-Weiss constant.

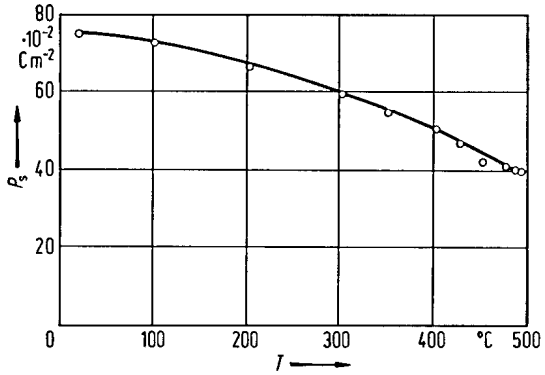

Fig. 1A-11-019. $PbTiO_3$. P_s vs. T [70Gav].

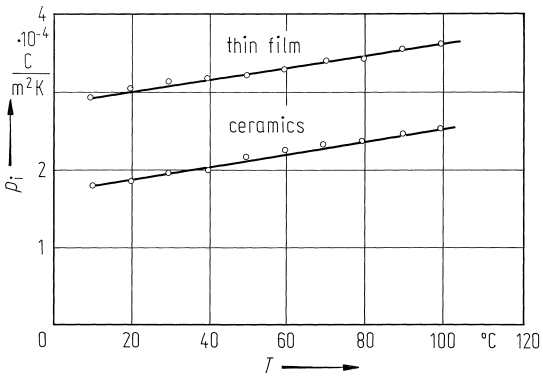

Fig. 1A-11-020. $PbTiO_3$ (thin film and ceramics). p_i vs. T [83Iij]. p_i: pyroelectric coefficient.

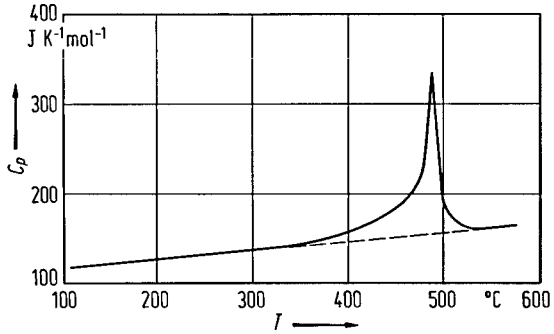

Fig. 1A-11-021. $PbTiO_3$. C_p vs. T [51Shi2]. C_p: molar heat capacity at constant pressure.

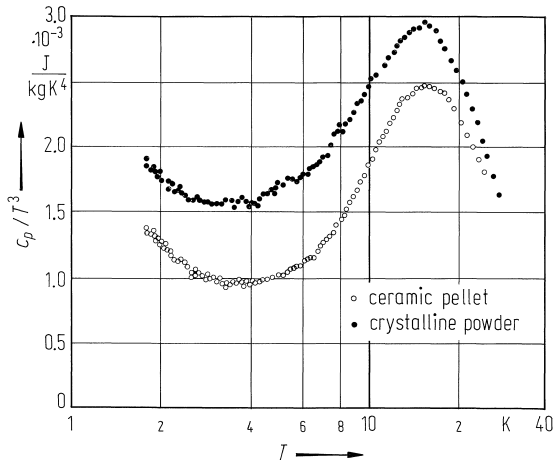

Fig. 1A-11-022. $PbTiO_3$. c_p/T^3 vs. T [83Law]. c_p: specific heat capacity at constant pressure.

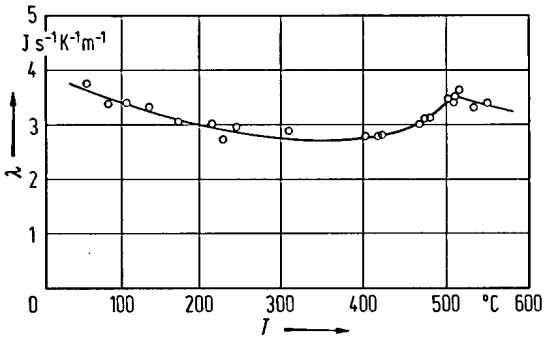

Fig. 1A-11-023. $PbTiO_3$. λ vs. T [60Yos]. λ: thermal conductivity.

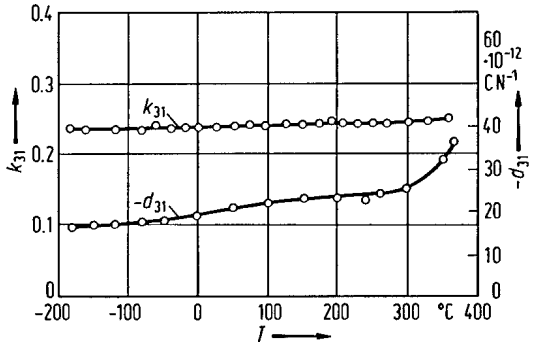

Fig. 1A-11-024. $PbTiO_3$. k_{31}, $-d_{31}$ vs. T [71Gav].

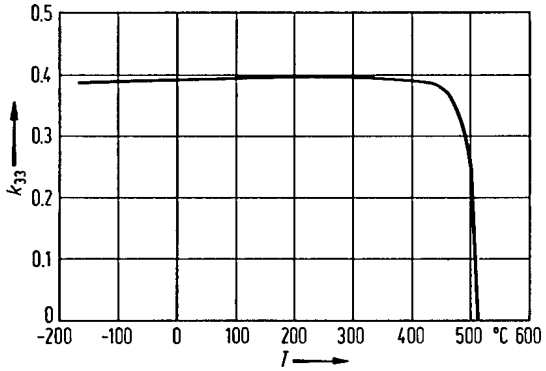

Fig. 1A-11-025. $PbTiO_3$ (ceramics). k_{33} vs. T [70Ike].

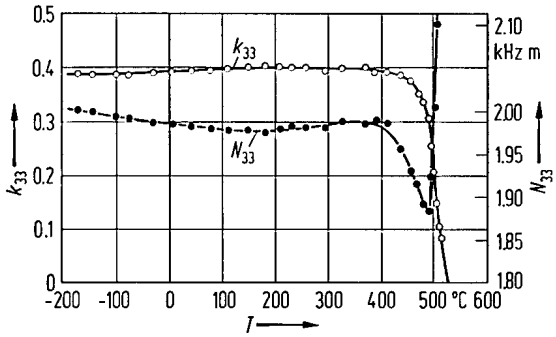

Fig. 1A-11-026. $PbTiO_3$ (ceramic with additive 1 mol% MnO_2). k_{33}, N_{33} vs. T [72Vie]. N_{33}: frequency constant.

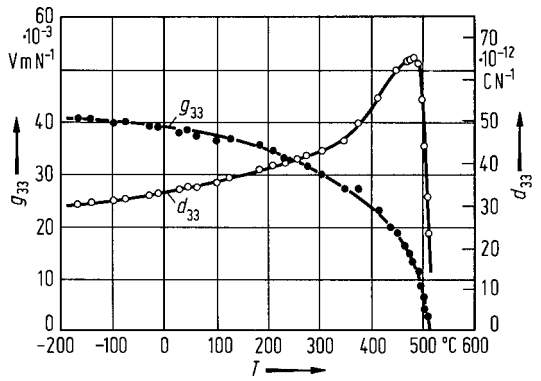

Fig. 1A-11-027. $PbTiO_3$ (ceramic with additive 1 mol% MnO_2). d_{33}, g_{33} vs. T [72Vie]. 1 V m N^{-1} = 1 m^2C^{-1}.

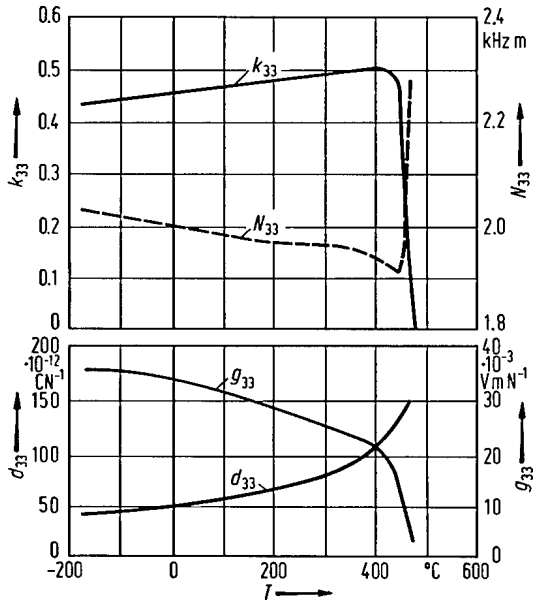

Fig. 1A-11-028. $PbTiO_3$ (ceramics containing La_2O_3 and MnO_2). k_{33}, N_{33}, d_{33}, g_{33} vs. T [71Ike]. N_{33}: frequency constant.

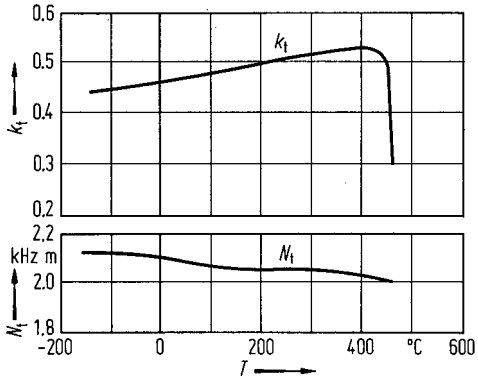

Fig. 1A-11-029. $PbTiO_3$ (ceramics containing La_2O_3 and MnO_2). k_t, N_t vs. T [71Ike]. k_t: thickness coupling factor, N_t: frequency constant (thickness vibration).

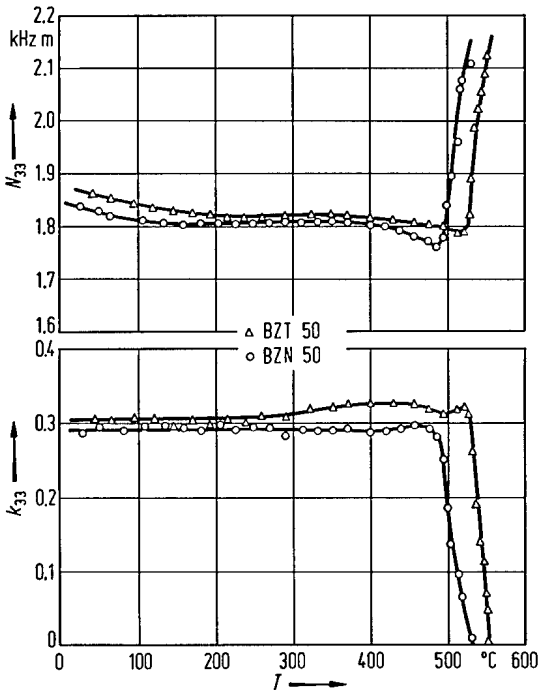

Fig. 1A-11-030. $PbTiO_3$ (ceramics). N_{33}, k_{33}, vs. T [68Ued]. N_{33}: frequency constant of the length extensional mode. BZT50: with additive $BiZn_{1/2}Ti_{1/2}O_3$, BZN50: with additive $Bi_{2/3}Zn_{1/3}Nb_{2/3}O_3$.

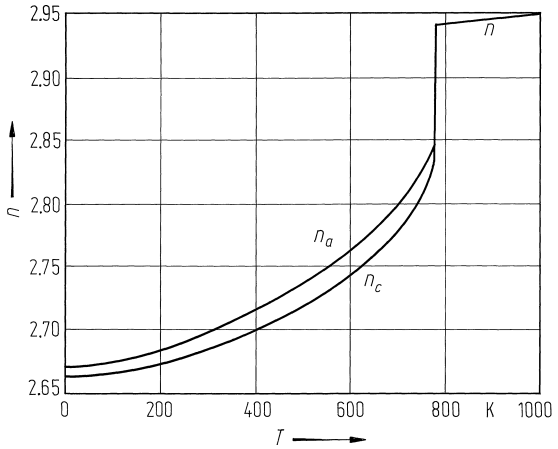

Fig. 1A-11-031. $PbTiO_3$. n_a, n_c, n vs. T [86Kle]. λ = 589.3 nm. n_a, n_c: refractive indices for E of light parallel to a and c.

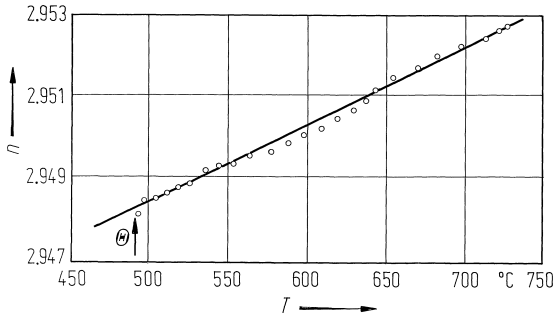

Fig. 1A-11-032. $PbTiO_3$. *n* vs. *T* [82Bur]. λ = 632.8 nm.

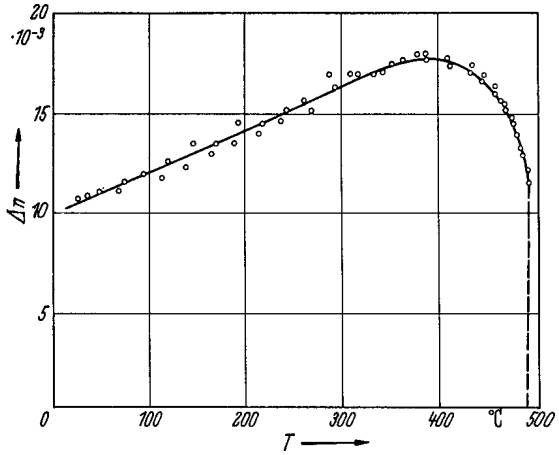

Fig. 1A-11-033. $PbTiO_3$. Δn vs. T [56Shi]. $\Delta n = n_a - n_c$. Na light was used.

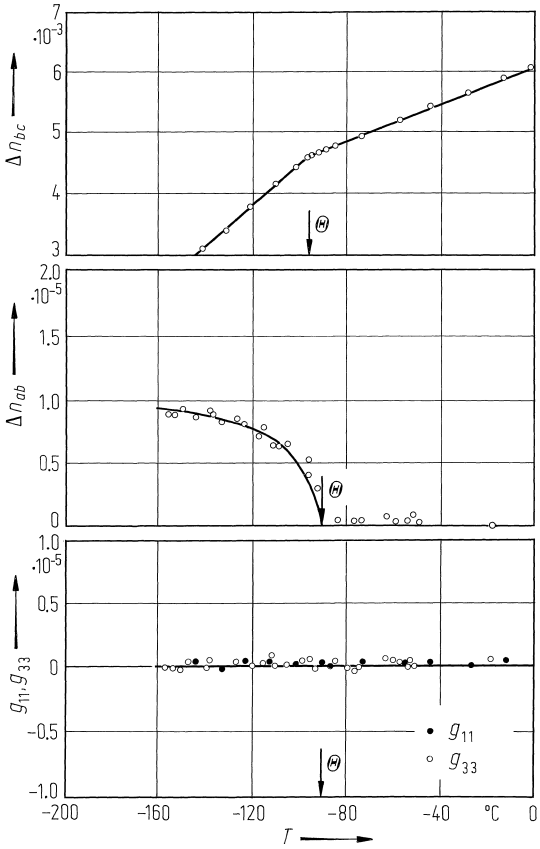

Fig. 1A-11-034. $PbTiO_3$. Δn_{bc}, Δn_{ab}, g_{11}, g_{33} vs. T [83Kob]. $\Delta n_{bc} = n_b - n_c$. $\Delta n_{ab} = n_a - n_b$. g_{11}, g_{33}: component of gyration tensor for optical activity.

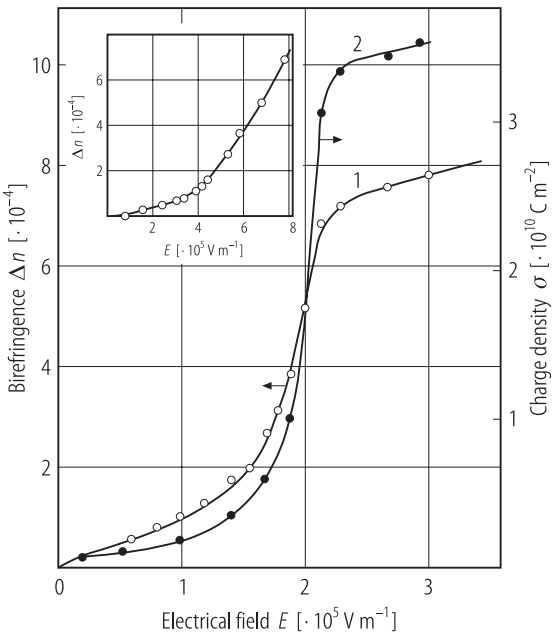

Fig. 1A-11-035. $PbTiO_3$. Δn, σ vs. E [90Che]. Δn: birefringence, σ: charge density, E: electric field.

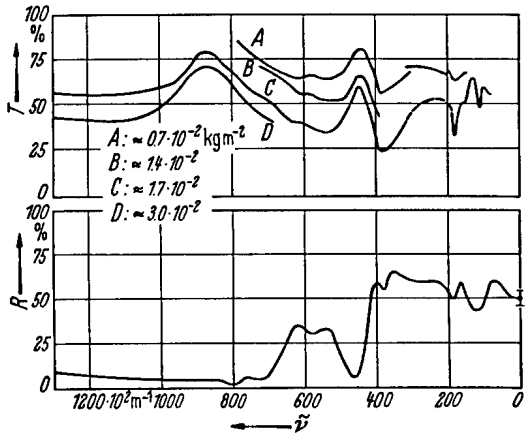

Fig. 1A-11-036. $PbTiO_3$. *T*, *R* vs. $\tilde{\nu}$ [64Per]. *T*: transmittance, *R*: reflectance, $\tilde{\nu}$: wave number. The $PbTiO_3$ concentrations of the samples are given in the figure.

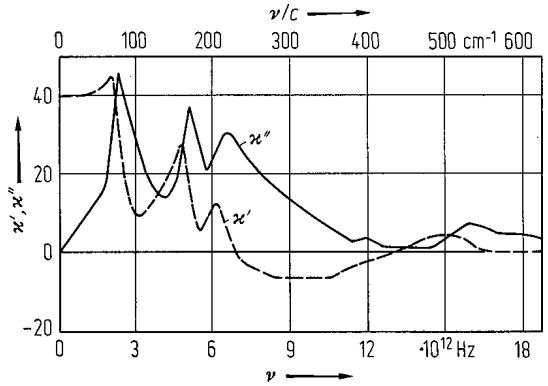

Fig. 1A-11-037. $PbTiO_3$. κ', κ'' vs. ν [64Per]. The curves were obtained from the reflectivity data using Kramers-Kronig relation.

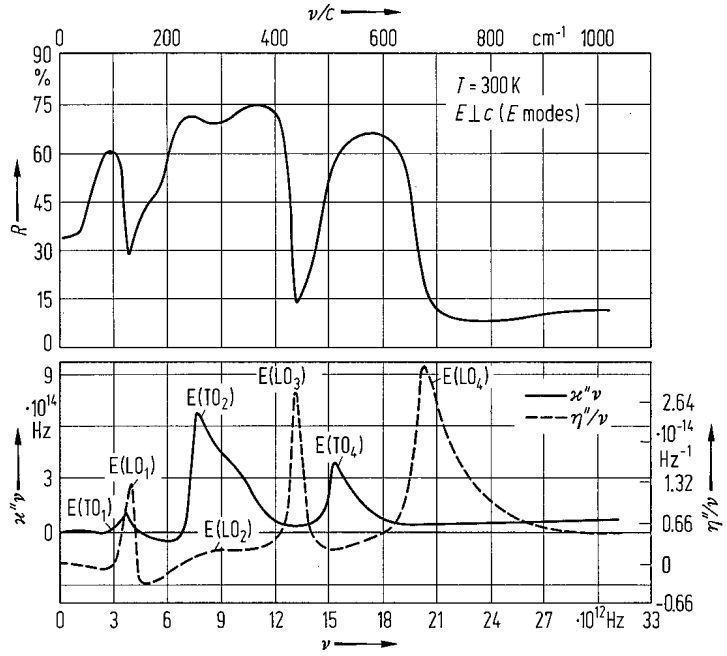

Fig. 1A-11-038. $PbTiO_3$. Infrared reflectance, conductivity, resistivity vs. ν [70Tor]. η": imaginary part of $1/\kappa$. Polarization of the incident light is normal to the *c*-axis (E-modes).

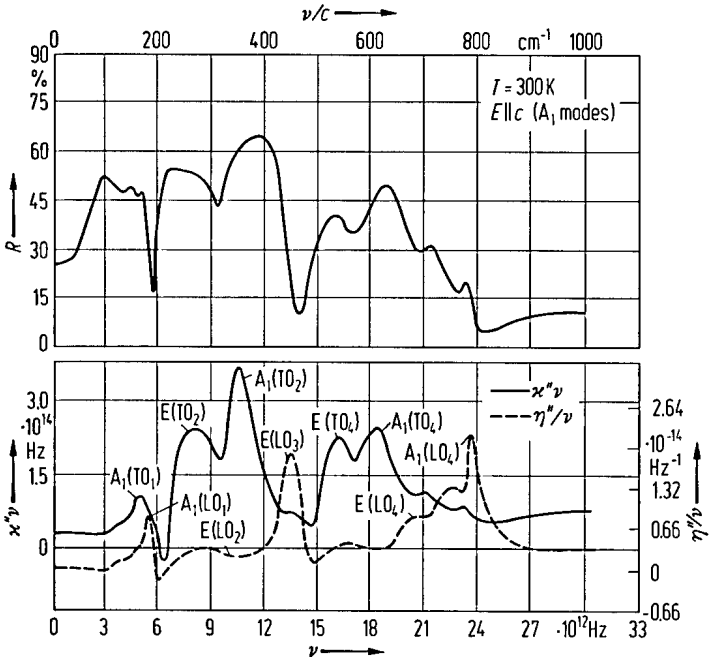

Fig. 1A-11-039. $PbTiO_3$. Infrared reflectance, conductivity, resistivity vs. ν [70Tor]. η'': imaginary part of $1/\kappa$. Polarization of the incident light is parallel to the *c*-axis (A_1-modes).

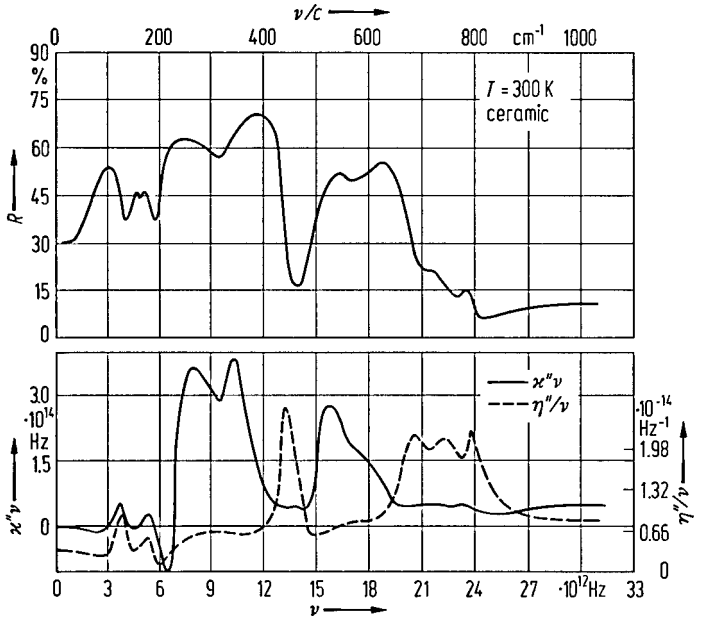

Fig. 1A-11-040. $PbTiO_3$ (ceramics). Infrared reflectance, conductivity, resistivity vs. ν [70Tor]. η": imaginary part of $1/\kappa$.

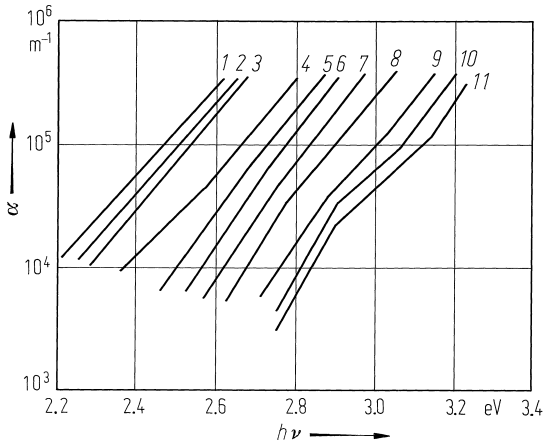

Fig. 1A-11-041. $PbTiO_3$. α vs. $h\nu$ [87Zam]. α: optical absorption coefficient. Parameter: *T*. Curve *1*: 856 °C, *2*: 802 °C, *3*: 760 °C, *4*: 758 °C, *5*: 680 °C, *6*: 645 °C, *7*: 589 °C, *8*: 526 °C, *9*: 425 °C, *10*: 343 °C, *11*: 293 °C.

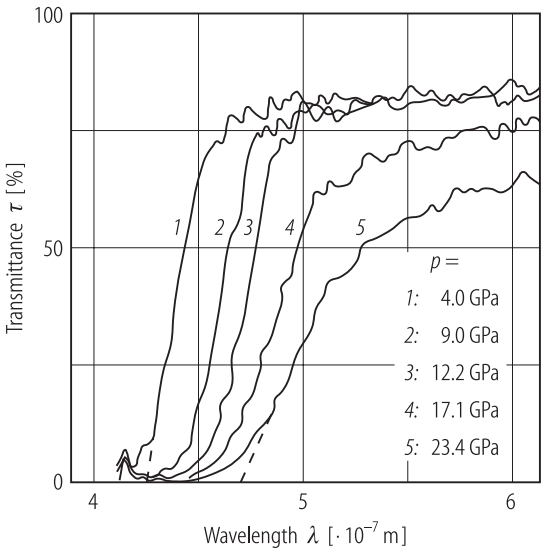

Fig. 1A-11-042. $PbTiO_3$. Transmittance τ vs. λ [92Zha].
λ: wavelength. Parameter: p.

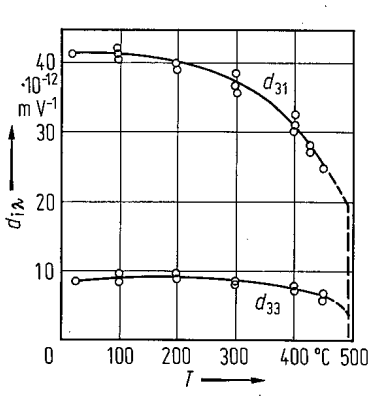

Fig. 1A-11-043. $PbTiO_3$. $d_{i\lambda}$ vs. T [77Ber]. $d_{i\lambda}$: nonlinear optical coefficient.

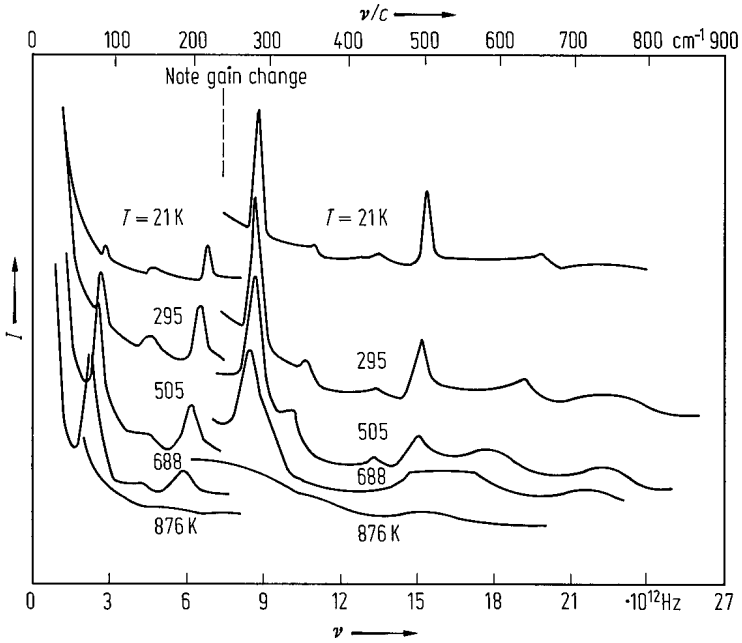

Fig. 1A-11-044. $PbTiO_3$. Raman spectra. Intensity vs. ν [70Bur]. Parameter: *T*.

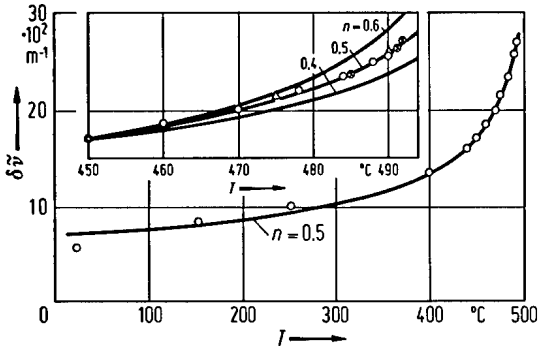

Fig. 1A-11-045. $PbTiO_3$. $\delta\tilde{\nu}$ vs. T [70Bur]. $\delta\tilde{\nu}$: Raman line width. The solid lines show the theoretical curves:

$$\delta\tilde{\nu} \propto \chi_{33}^{n} \propto \left[\left(1-\frac{3}{4}\frac{T-\Theta_p}{\Theta_f-\Theta_p}\right)+\left(1-\frac{3}{4}\frac{T-\Theta_p}{\Theta_f-\Theta_p}\right)^{\frac{1}{2}}\right]^{-n}$$

the best agreement with the experimental points occurs at $n = 0.5$.

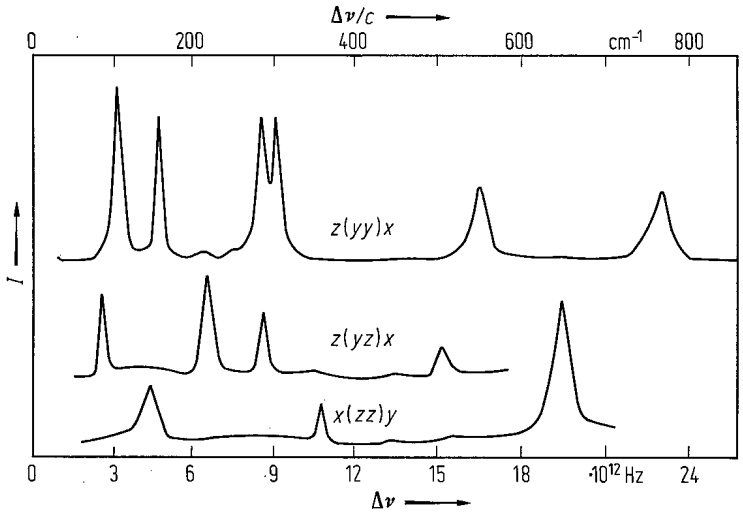

Fig. 1A-11-046. $PbTiO_3$. I vs. $\Delta\nu$ at RT [70Bur]. I: Raman scattering intensity. See also [73Fre].

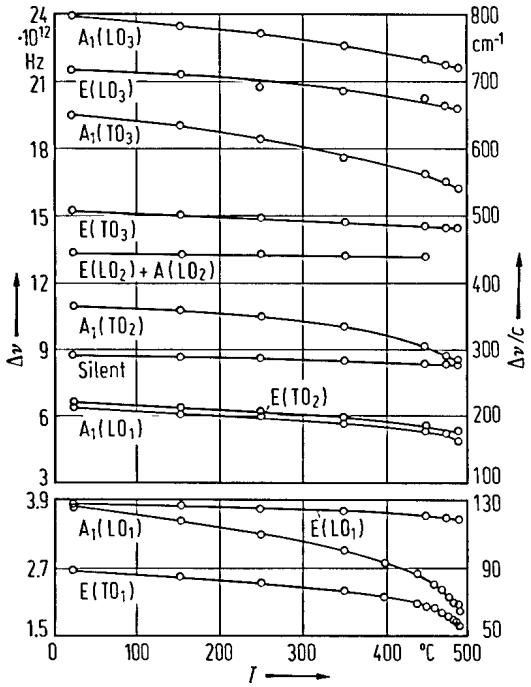

Fig. 1A-11-047. $PbTiO_3$. $\Delta\nu$ vs. T [73Bur]. $\Delta\nu$: Raman frequency shift.

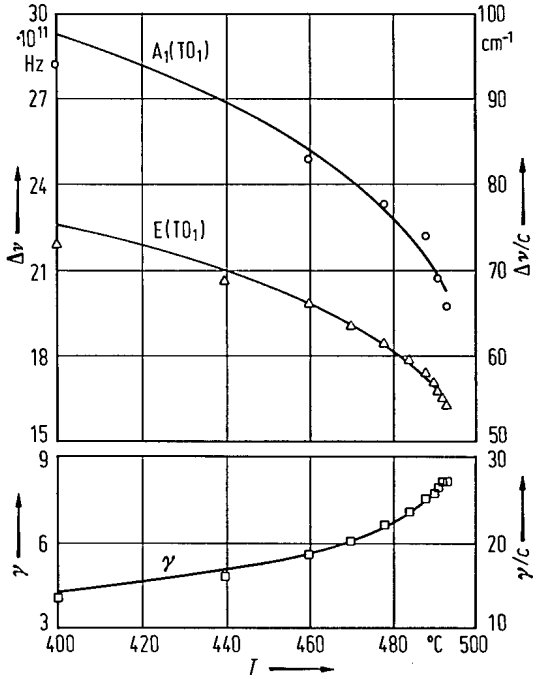

Fig. 1A-11-048. $PbTiO_3$. $\Delta\nu$, γ vs. T [73Bur]. $\Delta\nu$: Raman frequency shift of the lowest A_1 mode (open circles) and E mode (open triangles). γ: damping constant of the the lowest E mode. Solid lines are calculated results on an empirical model. See also [70Bur].

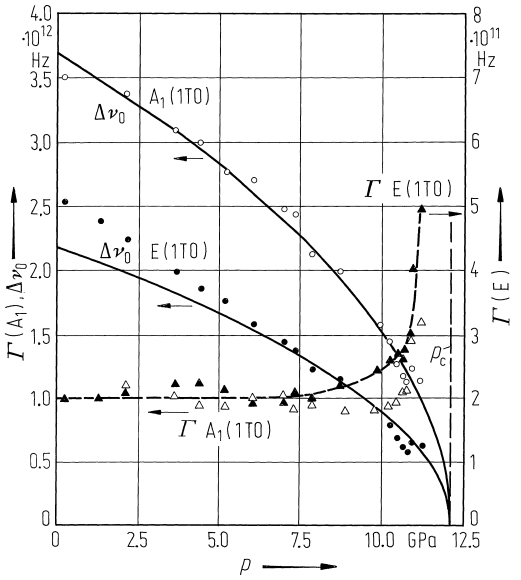

Fig. 1A-11-049. $PbTiO_3$. $\Delta\nu_0$, Γ vs. p [83San]. $\Delta\nu_0$: Raman shift, Γ: damping constant for the A_1 mode. Open circles and triangles: Raman shift and damping constant for A_1 mode. Full circles and triangles: Raman shift and damping constant for the E mode.

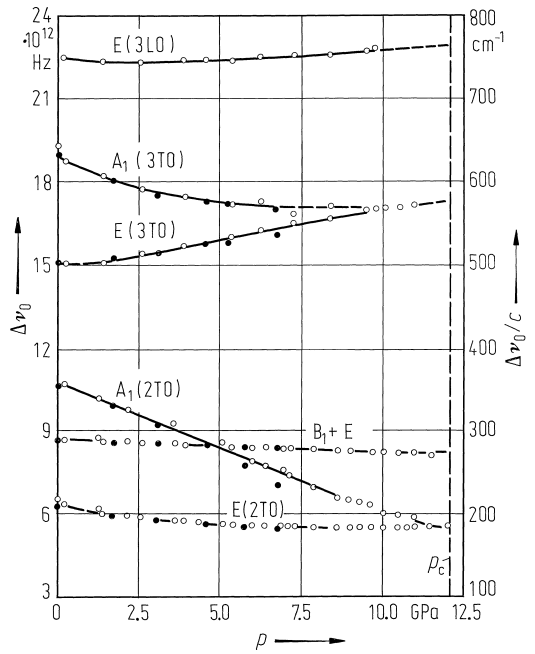

Fig. 1A-11-050. $PbTiO_3$. $\Delta\nu_0$ vs. p [83San]. $\Delta\nu_0$: Raman shift. Full circles: data from [75Cer]. nTO and nLO: n-th TO and LO modes.

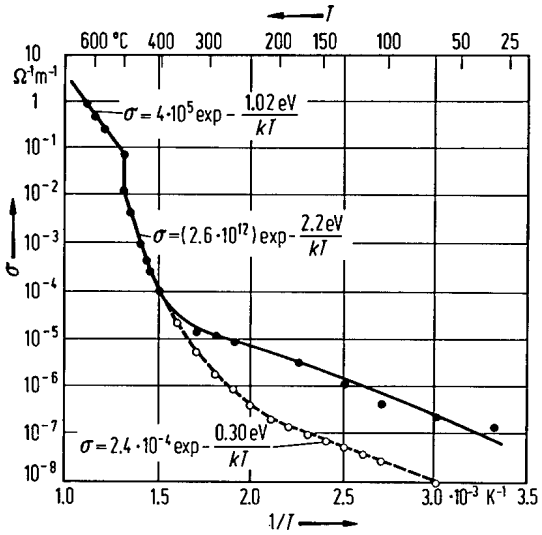

Fig. 1A-11-051. $PbTiO_3$. σ vs. T^{-1} [70Rem]. Open circles: dc conductivity, full circles: conductivity measured at 1 kHz, which includes the dielectric loss.

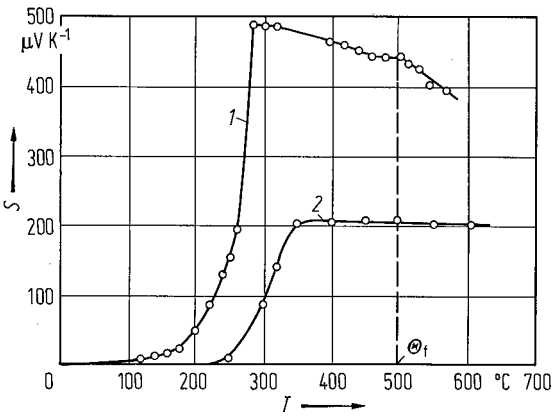

Fig. 1A-11-052. $PbTiO_3$. *S* vs. *T* [78Han]. *S*: Seebeck coefficient. Curve *1*: for single crystals highly reduced during the growing process, curve *2*: for single crystals unreduced.

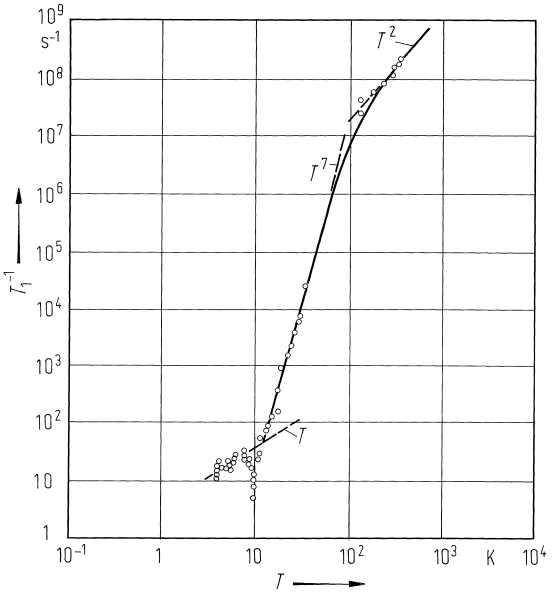

Fig. 1A-11-053. $PbTiO_3$ (ceramics). T_1^{-1} vs. T [86Bot]. T_1: spin-lattice relaxation time.

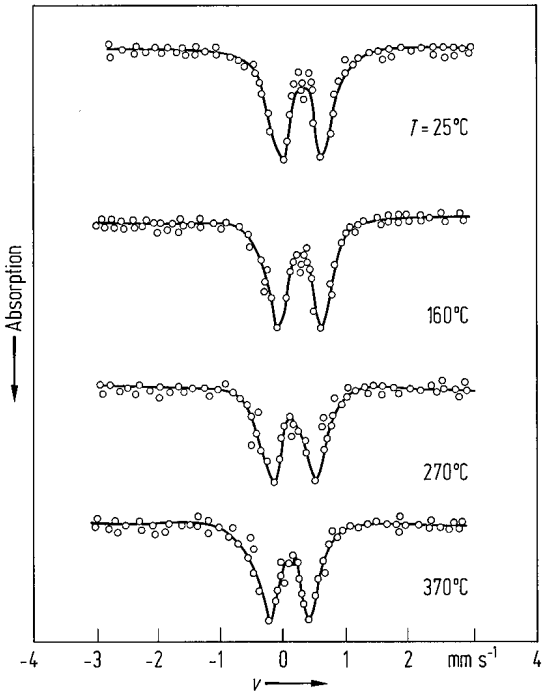

Fig. 1A-11-054. $PbTiO_3$: ^{57}Co. Mössbauer spectra [72Bhi]. Parameter: *T*. *v*: source velocity. The spectra matched against $K_4Fe(CN)_6 \cdot 3H_2O$ single crystal absorber.

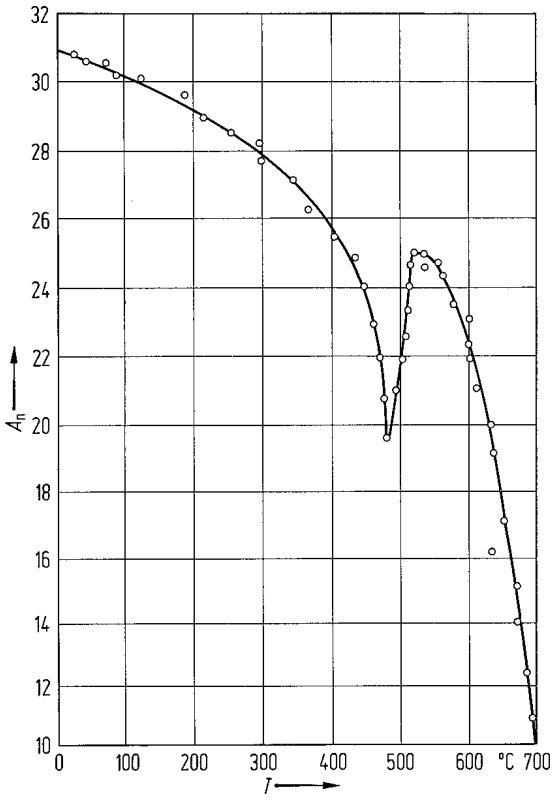

Fig. 1A-11-055. $PbTiO_3$: ^{57}Co. A_n vs. T [72Bhi].
A_n: normalized area of Mössbauer absorption spectrum.

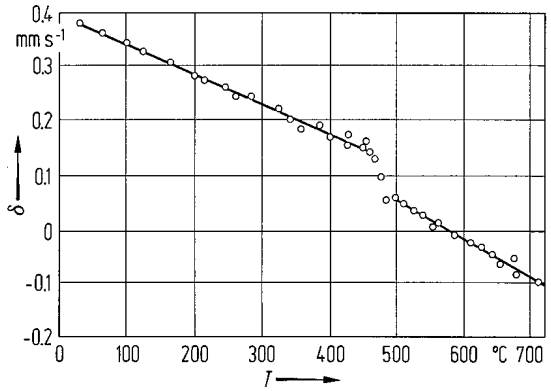

Fig. 1A-11-056. $PbTiO_3$: ^{57}Co. δ vs. T [72Bhi]. δ: isomer shift. The values are relative to 310 ESS absorber.

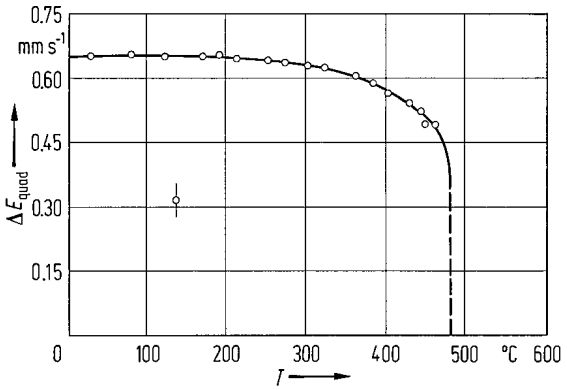

Fig. 1A-11-057. $PbTiO_3$: ^{57}Co. ΔE_{quad} vs. T [72Bhi].
ΔE_{quad}: quadrupole splitting.

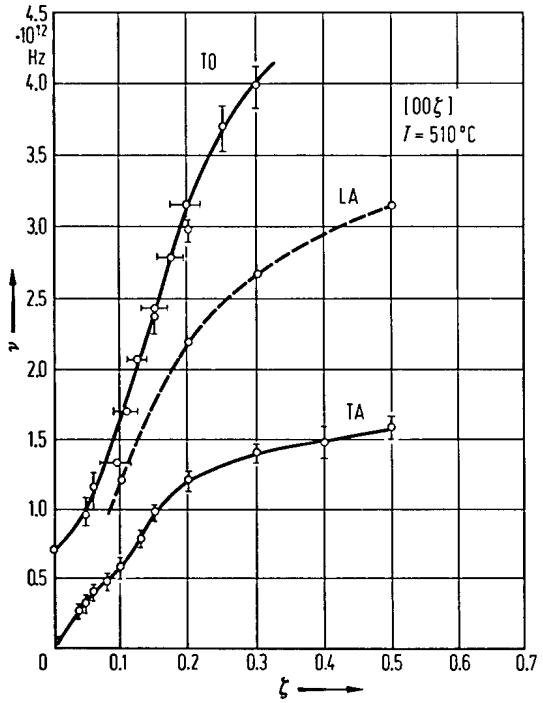

Fig. 1A-11-058. $PbTiO_3$. ν vs. ζ at 22 °C [70Shi]. ν: Phonon frequency, ζ: reduced wave vector coordinate. A single domain crystal was used, which was produced by the topseeded solution technique.

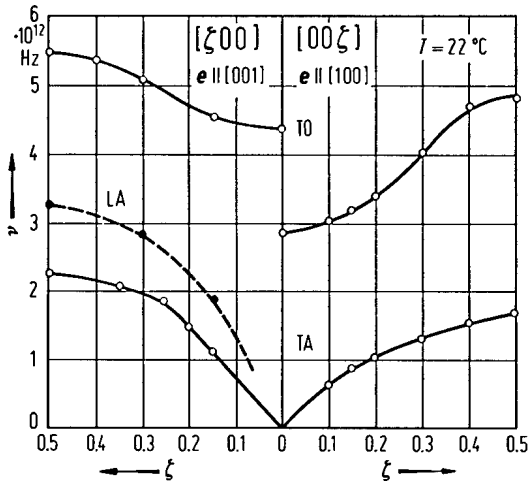

Fig. 1A-11-059. $PbTiO_3$. ν vs. ζ at 22 °C [70Shi]. ***e***: polarization vector. ν: Phonon frequency, ζ: reduced wave vector coordinate.

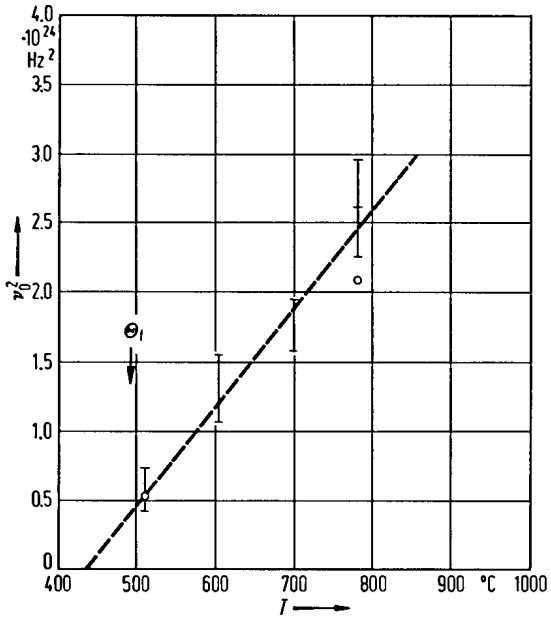

Fig. 1A-11-060. $PbTiO_3$. ν_0^2 vs. T [70Shi]. ν_0: frequency of lowest energy optic phonon at $q = 0$.

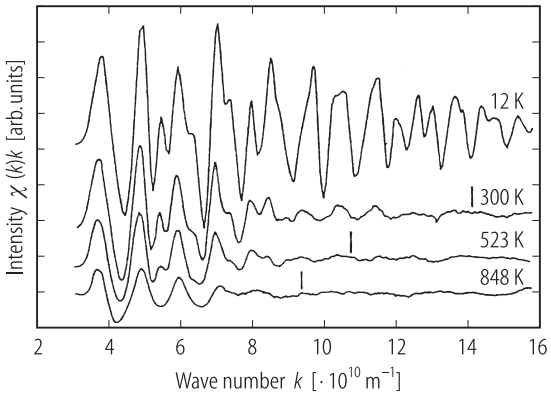

Fig. 1A-11-061. $PbTiO_3$. $\chi(k)$ k vs. k [94Sic]. $\chi(k)$ k: intensity (Pb edge), k: wave number.

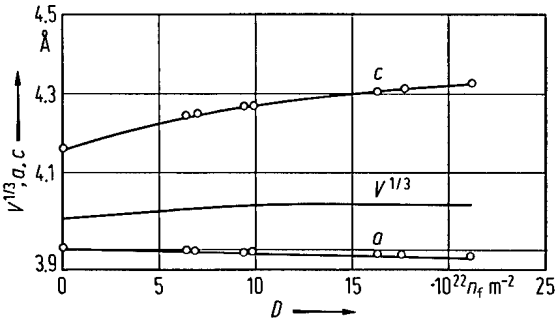

Fig. 1A-11-062. $PbTiO_3$. Lattice parameters vs. neutron dose, *D* [66Hau]. n_f: number of fast neutrons.

References

46Meg Megaw, H.D.: Proc. Phys. Soc. London **58** (1946) 133.
50Shi Shirane, G., Hoshino, S., Suzuki, K.: Phys. Rev. **80** (1950) 1105.
50Smo Smolenskii, G.A.: Dokl. Akad. Nauk SSSR **70** (1950) 405.
51Shi1 Shirane, G., Hoshino, S.: J. Phys. Soc. Jpn. **6** (1951) 265.
51Shi2 Shirane, G., Sawaguchi, E.: Phys. Rev. **81** (1951) 458.
52Nom Nomura, S., Sawada, S.: Rept. Inst. Sci. Technol. Univ. Tokyo **6** (1952) 191 (in Japanese).
52Rog Rogers, H.H.: Mass. Inst. Technol. Lab., Tech. Rep. Insulation Res. 1952, No. 56.
55Kob Kobayashi, J., Ueda, R.: Phys. Rev. **99** (1955) 1900.
56Kob Kobayashi, J., Okamoto, S., Ueda, R.: Phys. Rev. **103** (1956) 830.
56Shi Shirane, G., Pepinsky, R., Frazer, B.C.: Acta Crystallogr. **9** (1956) 131.
58Kob Kobayashi, J.: J. Appl. Phys. **29** (1958) 866.
59Kob Kobayashi, J., Yamada, N.: Mem. Sch. Sci. Eng., Waseda Univ. **23** (1959) 111.
59Ven Venevtsev, Yu.N., Zhdanov, G.S., Solov'ev, S.P., Ivanova, V.V.: Kristallografiya **4** (1959) 255; Sov. Phys. Crystallogr. (English Transl.) **4** (1959) 235.
60Yos Yoshida, I.: J. Phys. Soc. Jpn. **15** (1960) 2211.
61Ste Stetson, H., Schwartz, B.: J. Am. Ceram. Soc. **44** (1961) 420.
62Kab Kabalkina, S.A., Vereshchagin, L.F.: Dokl. Akad. Nauk SSSR **143** (1962) 818.
63Chr Christensen, A., Rasmussen, S.: Acta Chem. Scand. **17** (1963) 3.
64Gai Gainon, D.J.A.: Phys. Rev. **134** (1964) A1300.
64Per Perry, C.H., Khanna, B.N., Rupprecht, G.: Phys. Rev. **135** (1964) A408.
65Kuz Kuznetsov, V.A., Panteleev, V.V.: Kristallografiya **10** (1965) 445; Sov. Phys. Crystallogr. (English Transl.) **10** (1965) 369.
65Per Perry, C.H., McCarthy, D.J. Rupprecht, G.: Phys. Rev. **138** (1965) A1537.
66Hau Hauser, O., Schenk, M.: Phys. Status Solid **18** (1966) 547.
68Bhi Bhide, V.C., Hegde, M.S., Deshmukh, K.C.: J. Am. Ceram. Soc. **51** (1968) 565.
68Sht Shternberg, A.A., Kuznetsov, V.A.: Kristallografiya **13** (1968) 745; Sov. Phys. Crystallogr. (English Transl.) **13** (1969) 647.
68Ued Ueda, I., Ikegami, S.: Jpn. J. Appl. Phys. **7** (1968) 236.
69Gur Gurevich, V.M.: Elektroprovodnost' Segnetoelektrikov, Moskva: Izdatel'stvo Komiteta Standartov, Mer I Izmeritel'nykh Priboroy pri Sovete Ministrov SSSR, 1969; Electric Conductivity of Ferroelectrics, Jerusalem: Israel Program for Scientific Translations, 1971.
69Ike Ikegami, S., Ueda, I., Miyazawa, T.: J. Phys. Soc. Jpn. **26** (1969) 1324.
69Yam Yamada, Y., Shirane, G., Linz, A.: Phys. Rev. **177** (1969) 848.
70Bur Burns, G., Scott, B.A.: Phys. Rev. Lett. **25** (1970) 167.
70Gav Gavrilyachenko, V.G., Spinko, R.I., Martynenko, M.A., Fesenko, E.G.: Fiz. Tverd. Tela **12** (1970) 1532; Sov. Phys. Solid State (English Transl.) **12** (1970) 1203.
70Ike Ikegami, S., Ueda, I.: J. Phys. Soc. Jpn. **28** Suppl. (1970) 331.
70Rab Rabinovich, A.Z., Roitberg, M.B.: Kristallografiya **15** (1970) 1171; Sov. Phys. Crystallogr. (English Transl.) **15** (1970) 1023.
70Rem Remeika, J.P., Class, A.M.: Mater. Res. Bull. **5** (1970) 37.
70Shi Shirane, G., Axe, J.D., Harada, J., Remeika, J.P.: Phys. Rev. B **2** (1970) 155.
70Tak Takei, W.J., Formigoni, N.P., Francombe, M.H.: J. Vacuum Sci. Technol. **7** (1970) 442.
70Tor Tornberg, N.F., Perry, C.H.: J. Chem. Phys. **53** (1970) 2946.
71Gav Gavrilyachenko, V.G., Fesenko, E.G.: Kristallografiya **16** (1971) 640; Sov. Phys. Crystallogr. (English Transl.) **16** (1971) 549.
71Ike Ikegami, S., Ueda, I., Nagata, T.: J. Acoust. Soc. Am. **50** (1971) 1060.
71Pre Pressley, R.J. (ed.): CRC Handbook of Lasers, with selected Data on Optical Technology, Cleveland, chemical Rubber Co., (1971) p.452.
71Sam Samara, G.A.: Ferroelectrics **2** (1971) 277.

71Shi Shirasaki, S.: Solid State Commun. **9** (1971) 1217.
71Yag Yagnik, C.M., Gerson, R., James, W.J.: J. Appl. Phys. **42** (1971) 395.
71Yam Yamaka, E., Hayashi, T., Matsumoto, M.: Infrared Phys. **11** (1971) 247.
72Bhi Bhide, V.G., Hegde, M.S.: Phys. Rev. B **5** (1972) 3488.
72Fes Fesenko, E.G., Gavrilyachenko, V.G., Spinko, R.I., Martynenko, M.A., Grigoreva, E.A., Feronov, A.D.: Kristallografiya **17** (1972) 153; Sov. Phys. Crystallogr. (English Transl.) **17** (1972) 122.
72Sin Singh, S., Remeika, J.P., Potopowicz, J.R.: Appl. Phys. Lett. **20** (1972) 135.
72Ued Ueda, I.: Jpn. J. Appl. Phys. **11** (1972) 450.
72Vie Vieland, L.J.: J. Phys. Chem. Solids **33** (1972) 581.
73Bur Burns, G., Scott, B.A.: Phys. Rev. B **7** (1973) 3088.
73Dos Doshi, P., Class, J., Novotny, M.: Phys. Rev. B **7** (1973) 4260.
73Fes Fesenko, E.G., Gavrilyachenko, V.G., Martynenko, M.A., Semenchov, A.F., Lapin, I.P.: Ferroelectrics **6** (1973) 61.
73Fre Frey, R.A.: Proceedings of the 3rd International Conference on Raman Spectroscopy, held at Reims (1972); Advances in Raman Spectroscopy, Vol. 1, London: Heyden & Son. Ltd., 1973, p. 181.
73Shi Shirasaki, S., Takahashi, K., Kakegawa, K.: J. Am. Ceram. Soc. **56** (1973) 430.
74Dud Dudkevich, V.P., Tsikhotskii, E.S., Zakharchenko, I.N., Fesenko, E.G.: Fiz. Tverd. Tela **16** (1974) 3492; Sov. Phys. Solid State (English Transl.) **16** (1975) 2266.
75Cer Cerdeira, F., Holzapfel, W.B., Bauerle, D.: Phys. Rev. B **11** (1975) 1188.
75Ike Ikeda, T.: Solid State Commun. **16** (1975) 103.
75Shi Shirasaki, S. , Takahashi, K., Yamamura, H., Kakegawa, K., Mori, J.: J. Solid State Chem. **12** (1975) 84.
75Tan Tanaka, M.: Acta Crystallogr., Sect. A **31** (1975) 59.
76Fes Fesenko, E.G., Semenchev, A.F., Gavrilyatchenko, V.G.: Ferroelectrics **13** (1976) 471.
76Gra Grabmaier, B.C.: Ferroelectrics **13** (1976) 501.
76Hol Holman, R.L.: Ferroelectrics **14** (1976) 675.
76Lew Lewis, O., Wessel, G.: Phys. Rev. B **13** (1976) 2742.
76Mal Malitskaya, M.A., Martynenko, M.A., Popov, Yu.M., Prokopalo, O.I., Fesenko, E.G.: Fiz. Tverd. Tela **18** (1976) 1386; Sov. Phys. Solid State (English Transl.) **18** (1976) 798.
76Pro Prokopalo, O.I.: Ferroelectrics **14** (1976) 683.
76Yam Yamaka, E., Teranishi, A., Nakamura, K., Nagashima, T.: Ferroelectrics **11** (1976) 305.
77Ber Bergman, J.G., Crane, G.R., Turner, E.H.: J. Solid State Chem. **21** (1977) 127.
78Dud Dudkevich, V.P., Zakharchenko, I.N., Fesenko, E.G.: Ferroelectrics **18** (1978) 185.
78Gla Glazer, A.M., Mabud, S.A., Clarke, R.: Acta Crystallogr., Sect. B **34** (1978) 1060.
78Han Handerek, J., Wrobel, Z., Wojcik, K., Ujma, Z.: Ferroelectrics **18** (1978) 127.
78Hei Heiman, D., Ushida, S.: Phys. Rev. B **17** (1978) 3616.
79Mab Mabud, S.A., Glazer, A.M.: J. Appl. Crystallogr. **12** (1979) 49.
79Mal Malitskaya, M.A., Popov, Yu.M., Prokopalo, O.I., Raevskii, I.P., Rogach, E.D.: Fiz. Tverd. Tela **21** (1979) 2229; Sov. Phys. Solid State (English Transl.) **21** (1979) 1282.
79Oku Okuyama, M., Matsui, Y., Nakano, H., Nakagawa, T., Hamakawa, Y.: Jpn. J. Appl. Phys. **18** (1979) 1633.
80Tak Takashige, M., Nakamura, T., Ozawa, H., Uno, R., Tsuya, N., Arai, K.: Jpn. J. Appl. Phys. **19** (1980) L255.
81Lib Liberts, G.V., Fritsberg, V.Ya.: Phys. Status Solidi (a) **67** (1981) K81.
81Mat Matsui, Y., Okuyama, M., Fujita, N., Hamakawa, Y.: J. Appl. Phys. **52** (1981) 5107.
81Nak Nakamura, T., Takashige, M., Aikawa, Y.: J. Phys. (Paris) **42** (1981) Suppl. C–6, 421.
81Oku Okuyama, M., Matsui, Y., Nakano, H., Hamakawa, Y.: Ferroelectrics **33** (1981), 235.
81Roz Rozova, M.N., Onopko, D.E., Titov, S.A., Kostikov, Yu.P.: Fiz. Tverd. Tela **23** (1981) 1704; Sov. Phys. Solid State (English Transl.) **23** (1981) 992.

81Ter Terauchi, H., Tanabe, K., Maeda, H., Hida, M., Kamijo, N., Takashige, M., Nakamura, T., Ozawa, H., Uno, R.: J. Phys. Soc. Jpn. **50** (1981) 3977.
82Bur Burns, G., Dacol, F.H., Remeika, J.P., Taylor, W.: Phys. Rev. B **26** (1982) 2707.
83Iij Iijima, K., Kawashima, S., Ueda, I.: Proceedings of the 3rd Sensor Symposium, Tsukuba Science City, June 1983 (The Institute of Electrical Engineers of Jpn. Tokyo, 1983), p. 133.
83Kob Kobayashi, J.: Ferroelectrics **50** (1983) 53.
83Koj Kojima, M., Okuyama, M., Nakagawa, T., Hamakawa, Y.: Jpn. J. Appl. Phys. **22**, Suppl. 22–2 (1983) 14.
83Kup Kuprianov, M.F., Zaitsev, S.M., Gagarina, E.S., Fesenko, E.G.: Phase Transitions **4** (1983) 55.
83Law Lawless, W.N., Nakamura, T., Takashige, M., Swartz, S.L.: J. Phys. Soc. Jpn. **52** (1983) 207.
83Rae Raevskii, I.P., Malitskaya, M.A., Popov, Yu.M., Prokopalo, O.I., Servuli, V.A.: Fiz. Tverd. Tela **25** (1983) 1207; Sov. Phys. Solid State (English Transl.) **25** (1983) 692.
83San Sanjurjo, J.A., López-Cruz, E., Burns, G.: Phys. Rev. B **28** (1983) 7260.
83Shv Shveitser, I.G., Mazuritskii, M.I., Prokopalo, O.I.: Fiz. Tverd. Tela **25** (1983) 2273; Sov. Phys. Solid State (English Transl.) **25** (1983) 1305.
84Nak Nakamura, T., Takashige, M., Terauchi, H., Miura, Y., Lawless, W.N.: Jpn. J. Appl. Phys. **23** (1984) 1265.
85Bal Balachandran, R., Kutty, T.R.N.: J. Mater. Sci. Lett. **4** (1985) 898.
85Blu Blum, J.B., Gurkovich, S.R.: J. Mater. Sci. **20** (1985) 4479.
85Nad Nadolinskaya, E.G., Smolenskii, G.A., Shil'nikov, A.V., Yushin, N.K.: Fiz. Tverd. Tela **27** (1985) 2215; Sov. Phys. Solid State (English Transl.) **27** (1985) 1996
85Shi Shiosaki, T., Adachi, M., Mochizuki, S., Kawabata, A.: Ferroelectrics **63** (1985) 227.
86Bot Böttcher, R., Brunner, W., Milsch, B., Völkel, G., Windsch, W., Kirillov, S.T.: Chem. Phys. Lett. **129** (1986) 546.
86Iij Iijima, K., Tomita, Y., Takayama, R., Ueda, I.: J. Appl. Phys. **60** (1986) 361.
86Kle Kleemann, W., Schäfer, F.J., Rytz, D.: Phys. Rev. B **34** (1986) 7873.
86Nel Nelmes, R.J., Katrusiak, A.: J. Phys. C **19** (1986) L725.
87Mal Malitskaya, M.A., Raevskii, I.P., Popov, Yu.M., Fridkin, V.M., Chervonobrodov, S.P., Chernenko, N.V.: Fiz. Tverd. Tela **29** (1987) 565; Sov. Phys. Solid State (English Transl.) **29** (1987) 322.
87Zam Zametin, V.I., Yakubovskii, M.A., Kosyanko, M.Yu.: Fiz. Tverd. Tela **29** (1987)1312; Sov. Phys. Solid State (English Transl.) **29** (1987) 751.
90Che Chervonobrodov, S.M., Fridkin, V.M., Malitskaya, M.A., Raevskii, I.P.: Ferroelecrics **103** (1990) 67.
92Pro Prosandeyev, S.A., Tarasevich, Yu.Y., Teslenko, N.M.: Ferroelecrics **131** (1992) 137.
92Zha Zha, C.S., Kalinichev, A.G., Bass, J.D., Suchicital, C.T.A., Payne, D.A.: J. Appl. Phys. **72** (1992) 3705.
93Tab Tabata, H., Murata, O., Kawai, T., Okuyama, M.: Jpn. J. Appl. Phys. **32** (1993) 5611.
93Sun Sun, B.N., Huang, Y., Payne D.A.: J. Cryst. Growth **128** (1993) 867.
94Gav Gavrilyatchenko, V.G., Semenchov, A.F., Fesenko, E.G.: Ferroelectrics **158** (1994) 31.
94Kin King-Smith, R.D., Vandorbilt, D.: Phy. Rev. B **49** (1994) 5828.
94Sic Sicron, N., Ravel, B., Yacoby, Y., Stern, E.A., Pogen, F., Rehr, J.J.: Phy. Rev. B **50** (1994) 13168.
95Fon Fontana, M.D., Abdi, F., Wojcik, K.: J. Appl. Phys. **77** (1995) 2102.